ORIGINAL ARTICLE

Taylor&Francis healthsciences

Quality Assurance of Patient Dosimetry in Boron Neutron Capture Therapy

Per M. Munck af Rosenschöld, Jacek Capala, Crister P. Ceberg, Valerio Giusti, Leif G. Salford and Bertil R.R. Persson

From the Departments of Medical Radiation Physics, Lund University (P.M. Munck af Rosenschöld, C.P. Ceberg, B.R.R. Persson), Biomedical Radiation Sciences, Uppsala University (J. Capala), Neurosurgery (Rausing Laboratory), Lund University (L.G. Salford), Sweden and Mechanical, Nuclear and Production Engineering, Pisa University, Italy (V. Giusti)

Correspondence to: Per M. Munck af Rosenschöld, Dept. of Radiation Physics, Lund University Hospital, Klinikgatan 7, 221 85 Lund, Sweden. Tel: +46 46 17 39 93. Fax: +46 46 13 61 56. E-mail: per.munck@skane.se

Acta Oncologica Vol. 43, No. 4, pp. 404–411, 2004

The verification of the correctness of planned and executed treatments is imperative for safety in radiotherapy. The purpose of the present work is to describe and evaluate the quality assurance (QA) procedures for patient dosimetry implemented at the boron neutron capture therapy (BNCT) facility at Studsvik, Sweden. The dosimetric complexity of the mixed neutron–photon field during BNCT suggests a careful verification of routine procedures, specifically the treatment planning calculations. In the present study, two methods for QA of patient dosimetry are presented. The first is executed prior to radiotherapy and involves an independent check of the planned absorbed dose to be delivered to a point in the patient for each treatment field. The second QA procedure involves in vivo dosimetry measurements using post-treatment activation analysis. Absorbed dose conversion factors taking the difference in material composition and geometry of the patient and the PMMA phantom used for reference dosimetry were determined using the Monte Carlo method. The agreement of the QA procedure prior to radiotherapy reveals an acceptably small deviation for 60 treatment fields of ±4.2% (1 SD), while the in vivo dosimetry method presented may benefit from improvements, as the deviations observed were quite substantial (±12%, 1 SD), and were unlikely to be due to actual errors in the clinical dosimetry.

Received 4 August 2003
Accepted 10 March 2004

A facility designed for the delivery of boron neutron capture therapy (BNCT) has been built at the research reactor at Studsvik, Sweden (1–3). The topic of BNCT was recently reviewed (4). In BNCT, the patient is exposed to a mixed radiation field of neutrons and photons. Photons, produced in neutron interactions, and their progeny give rise to the photon absorbed dose component, while neutron interactions producing charged particles give rise to the neutron absorbed dose component. The various neutron interactions giving rise to absorbed dose in tissue are generally treated separately, where proton recoils from neutron scatter in hydrogen (referred to as the fast neutron dose), as well as neutron capture in boron and nitrogen (referred to as boron and nitrogen dose, respectively), are clinically relevant.

Owing to the different biological effectiveness of the mixed field components (5), an individual quantification under reference conditions is required. The subject of dosimetry of epithermal neutron beams has been presented by other authors previously (6–9) and has been discussed separately for the Studsvik facility (10, 11). In the present clinical trial at the Studsvik facility, the TPS is used to derive PMMA-to-patient absorbed dose conversion factors, implying that the TPS can take differences in material composition and geometry into account properly. Reference phantom to patient absorbed dose ratios typically deviate quite substantially from unity in the epithermal neutron beams; dosimetric studies of geometrical and material effect have been performed (9, 12–14). Some details were given previously of the clinical dosimetry methods used at the facility (2); a complete investigation is presently being prepared for separate publication. Safety and efficacy in radiotherapy require verification of the planned and delivered radiation absorbed dose to each individual patient (15–17), and this was recently made compulsory by national law. Radiotherapy should be verified using a detector that provides relevant information on the absorbed dose delivered to the patient. Preferably, the in vivo dosimetry procedure should give a direct measure of the delivered dose without corrections, which can be compared with the primary dosimetry system, i.e. the TPS. Ideally, the measurements should give on-line information on the

 ISSN 0284-186X
DOI: 10.1080/02841860410031390

delivered absorbed dose enabling the medical physicist to monitor the treatment. Finally, the detector or detectors should not cause a significant alteration of the planned dose distribution. In theory, the prompt gamma spectroscopy (PGS) method satisfies the criteria for BNCT, as it allows on-line monitoring of both the boron uptake and the thermal neutron fluence rate through the 478 keV gammas from boron and the 2.22 MeV gammas from hydrogen (18–20). The PGS method is a costly and complicated system to set up, and is beset by practical problems (18–20). There is for this reason an apparent need for a simpler and less costly in vivo dosimetry system for use in clinical BNCT.

The use of activation detectors as in vivo dosimeters has been successfully implemented in fast neutron therapy as entrance, exit, and intracavitary absorbed dose monitors (21). Activation detectors have been used in BNCT and preliminary data have been reported for the facility in Petten, The Netherlands; however, only variations in the activity of foils placed on the patient's skin for the four fractions used in the treatment were reported without discussion on the clinical implications of the measurements (22). A method for in vivo dosimetry was reported for an animal study performed using the epithermal neutron beam at the BNCT facility located in Helsinki, Finland, which could be regarded as the first report on the topic (23, 24). In that study thermoluminescent dosimeters (TLDs) and activation foils were used on multiple positions on the animals and comparisons were made with the measured and TPS-calculated photon absorbed doses and neutron fluence rates, respectively. Substantial deviations between measurements and calculations were observed, particularly for the TLD measurements (24).

An inherent problem of using activation wires is that the information is acquired in a post-treatment analysis, in contrast with 'on-line' measurements. Thus, possible errors in the treatment-planning calculations will be observed too late, which raises the need for an additional quality assurance (QA) procedure prior to therapy. Undoubtedly, it is recommendable to execute an independent QA procedure of the planned treatment well before the delivery of radiotherapy regardless of how the in vivo dosimetry system operates. In the present study, we suggest a novel approach for the QA of patient dosimetry in BNCT. The primary focus of this study is verification of the absorbed dose delivered to the dose-limiting organ (healthy brain tissue), rather than radioprotection of the patient. This perspective is taken on the basis of the patient group considered under the present protocol at the BNCT facility in Studsvik that has been diagnosed with glioblastoma multiforme (2), a group of patients proved to have a poor prognosis (25). The design, implementation, and evaluation of an in vivo dosimetry system and a dosimetric QA procedure prior to therapy are equally important objectives of the present study. A complete discussion about the QA of a BNCT facility is beyond the scope of the present study.

MATERIAL AND METHODS

In the present study, an analytical Snyder head model was chosen as an approximation of a human head, because of its simplicity to simulate using a Monte Carlo code. Kiger et al. (26) used the same analytical description previously. However, in this study scalp and skull compartments were also introduced, both of 5 mm thickness. MCNP code version 4c2 (27) was used to simulate the geometries depicted in Fig. 1. The calculations were used for the two aspects of absorbed dose verification investigated in the present study.

Independent verification of treatment planning calculations

The absorbed dose to the patient at the dose maximum for a single treatment field for each dose component (index i) can be written as

$$D_{i,\,pat} = \left(\frac{D_{i,\,sny}}{D_{i,\,PMMA}}\right)_{MC} \cdot \frac{D_{i,\,PMMA}}{M} \cdot M \qquad [1]$$

where $D_{i,PMMA}/M$ denotes the dose-per-monitor unit ratio measured under reference conditions (11), M denotes the total number of monitor units for the particular treatment field of interest, and the $(D_{i,sny}/D_{i,PMMA})_{MC}$ ratio is a Monte Carlo calculated factor that converts the absorbed dose measured under reference conditions to the absorbed dose at the maximum in the patient situation. The factor corrects for differences in the geometric and material composition of the PMMA phantom and the patient. It is assumed that the absorbed dose to the modified Snyder head model depicted in Fig. 1 and the patient are equal. Figure 1 depicts the different geometries investigated; they constitute two typical cases of irradiation geometry (e.g. 'Side' and 'Top'), which means that there will be two sets of the $(D_{i,sny}/D_{i,PMMA})_{MC}$ ratio. The distance of the irradiated object from the collimator will also have an impact on the absorbed dose rate. However, this effect was omitted in the present application as all patients were irradiated with a skin-to-collimator distance between 0 and 1 cm. For the boron dose component linear scaling was introduced to convert the 25 μg/g B-10 boron dose to that of the actual concentration at the time of treatment. A boron concentration in the skin compartment of 1.5 times the concentration in the healthy brain tissue was assumed (28), i.e. 37.5 μg/g. The sum of the absorbed dose of each component calculated to the maximum in this fashion is subsequently referred to as the 'reference dose value'. The absorbed dose components are weighted according to their respective biological effectiveness and added together as described and motivated in the present clinical protocol. The procedure for calculating a total weighted absorbed dose has also been described in some detail in an IAEA technical report (29). The biological weighting factor applied was the

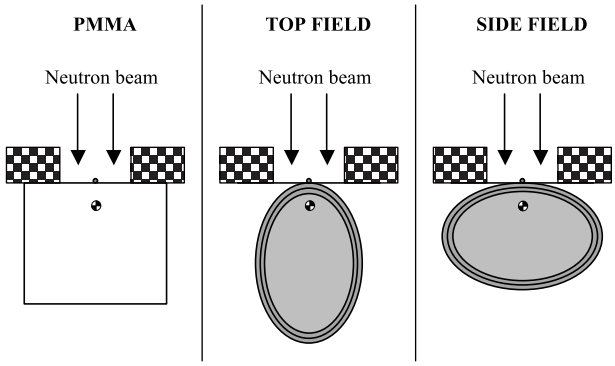

Fig. 1. Schematic view from above of the MCNP models that were simulated in the present work. The checkered areas are the beam collimators made of a polyethylene–boron–lead mixture. The picture to the left shows schematically the geometry for the calculation of absorbed dose to PMMA ($D_{i,PMMA}$) and the wire activity (A_{PMMA}), respectively. The pictures in the centre and to the right show the geometry of the ellipsoidal head model made of ICRU brain tissue with 25 μg/g ^{10}B with scalp and skull compartments added (both 5 mm thick with boron-10 concentrations of 37.5 μg/g and zero, respectively). The activation wire was positioned in the centre of the 10×14 cm^2 beam aperture, and noted by a small dot on the surface of the phantoms. The point on the beam axis on 3 cm depth is chosen as the reference point (entrance dose point), marked: ◓

following (applicable to healthy brain tissue): photon dose: 1.0, boron dose: 1.3, nitrogen dose: 3.2, fast neutron dose (proton recoil): 3.2 (5). The absorbed dose for each component calculated by the TPS at the dose maximum was extracted and compared with the 'reference dose value' for each treatment field. Data from the first 30 patients treated were collected (each patient was treated with two fields). The patients' treatment plans were made using a Monte Carlo based TPS called SERA, previously described in the literature (30–32).

In vivo dosimetry

The activity (A) of the product nuclide with the decay constant (λ) per gram of the sample, exposed to a constant neutron fluence rate of (ϕ), at the end of an irradiation time length of (t) can be written as:

$$A = \int_E \phi(E)\cdot\sigma(E)\cdot a\cdot(1 - e^{-\lambda\cdot t})dE \qquad [2]$$

where a is the number of atoms of the activation nuclide per gram of the sample with a cross-section of σ, and where E is the neutron energy. If we now consider gold and copper as the nuclides of interest we can Taylor expand the expression since λ times t will be close to zero; gold has a half-life of 2.695 days and copper has a half-life of 12.71 hours and t is in the order of 5–15 minutes at the BNCT facility in Studsvik, giving:

$$A = (1 - 1 + \lambda\cdot t + \ldots)\cdot \int_E \phi(E)\cdot\sigma(E)\cdot a\cdot dE$$
$$\approx \lambda\cdot t\cdot \int_E \phi(E)\cdot\sigma(E)\cdot a\cdot dE \qquad [3]$$

This means that the activity induced in the wire will be proportional to the neutron fluence rate (ϕ) times the irradiation time (t), i.e. the total neutron fluence. In the case that the neutron fluence is not constant with time the induced activity will still be proportional to the total neutron fluence as long as t is short compared with the half-life. As the activity of an activation wire is proportional to the neutron fluence, and the neutron fluence is proportional to the neutron dose, it is reasonable to suggest the use of a small activation wire for in vivo dosimetry use. Furthermore, it is also such that the photon dose is strongly dependent on the neutron fluence in epithermal neutron beams. This is due to the fact that a substantial fraction of the photons in hydrogenous material, such as body tissues, derive from radiative neutron capture in hydrogen; H(n,γ)D. From the above arguments it is clear that the activity of an activation wire holds relevant information of all absorbed dose components present in a BNCT beam. Though the activation wire can give information on the neutron fluence, no information is given on the material composition in the patient (specifically the boron uptake and the nitrogen concentration). In the present work we assume that the boron uptake is known through the use of ICP-AES (inductive coupled plasma atomic emission spectroscopy).

In the present study we have chosen to use a gold-copper activation wire as an in vivo dosimeter. The wire was positioned on the surface of the reference phantom and calibrated against each absorbed dose component at 3 cm depth in the reference PMMA phantom on the beam centreline. This gives a dose-per-activity ratio applicable for the phantom situation. Then, the same parameters can be related to the patient situation through Monte Carlo simulations taking both geometrical and material effects into account. We can write:

$$\frac{D_{i,pat}}{A_{pat}} = \left(\frac{D_{i,sny}}{A_{sny}} \cdot \frac{A_{PMMA}}{D_{i,PMMA}}\right)_{MC} \cdot \frac{D_{i,PMMA}}{A_{PMMA}} \quad [4]$$

where $D_{i,PMMA}/A_{PMMA}$ denotes the absorbed dose and activity ratio determined under reference conditions (11), $D_{i,pat}/A_{pat}$ denotes the dose-per-activity ratio for the patient situation, and the $((D_{i,sny}/A_{sny})\cdot(A_{PMMA}/D_{i,PMMA}))_{MC}$ factor that converts the absorbed dose per activity ratio measured under reference conditions to the patient situation (which is influenced by geometric factors and differences in material composition). The activity refers to the measured activity of a wire placed on the surface of the phantom or the patient, respectively (see Fig. 1), while the absorbed doses refers to a position at 3 cm depth on the beam axis (which is the dose maximum). In equation 4 it is assumed that the ratio of absorbed dose and activity in the modified Snyder model ($D_{i,sny}/A_{sny}$) is identical to the absorbed dose and activity ratio in the in the patient. A_{pat} was obtained from an activation wire for each individual treatment field at the time of the therapy. A high-purity germanium crystal was used to determine the gold and copper activities of the activation wires. The possibility of calculating the $((D_{i,sny}/A_{sny})\cdot(A_{PMMA}/D_{i,PMMA}))_{MC}$ factor using the TPS was not utilized due to its simplistic treatment of the gold resonance (5 eV) (i.e. it makes use of binned cross-sections), which could be of importance in the present application. The MCNP library used was continuous (ENDF60) (27), and in addition, using the MCNP code allowed development of QA systems that were independent from the TPS, which is preferable.

RESULTS AND DISCUSSION

Independent verification of treatment planning calculations

The absorbed dose at 3 cm depth in the reference phantom made of PMMA (Perspex^{TM}) is given in Table 1 (11). The results of the MCNP calculations performed in this study are presented in Table 2. The activation rate for the ^{197}Au $(n,\gamma)^{198}$Au – reaction was calculated using the ENDF/B-VI libraries, while activation rate [2] is calculated using the (binned) dosimetry libraries of MCNP version 4c2 (see Table 2). The boron and nitrogen (thermal neutron) doses are not defined in the PMMA phantom, as this material does not contain these elements. The absorbed dose in brain tissue and PMMA is different due to the different material composition, primarily due to the different hydrogen and boron concentrations (13). The photon absorbed dose was lower in the ellipsoidal brain for geometric reasons, i.e. less scattering material in the close vicinity of the reference point at 3 cm point results in less capture gammas generated, which means that photon absorbed dose is lower in the 'Top' field than in the 'Side' field. This was also the reason for the lower thermal neutron fluence in the 'Top' field than in the 'Side' field. The fast neutron absorbed dose was higher in brain tissue at 3 cm depth than in PMMA due to a higher hydrogen concentration.

Table 1

Summary of measured absorbed dose rate and per monitor unit (M) to the PMMA phantom at 3 cm depth, on the beam centreline and with a distance of 0 cm between the collimator and the phantom. The absorbed dose components were measured at 300 kW reactor power (the maximum reactor power is 1 MW). The thermal neutron group fluence (0–0.414 eV) at the same point in the PMMA phantom was 4.93×10^5 cm^{-2}MU^{-1} and $1.86 \cdot 10^9$ cm^{-2}s^{-1}

Absorbed dose component	Gy/MU	Gy/h
Photon	4.79×10^{-7}	6.62
Fast neutron	2.91×10^{-8}	0.40

In the present calculations we have used the boron concentration of 25 μg/g. A different boron concentration will influence the neutron fluence, particularly the thermal neutron part of the spectra due to the high thermal cross-section of boron. This will in turn affect both the nitrogen and hydrogen reaction rates to some extent. These effects are ignored in the present application. The average of the boron concentration in the blood during treatment for the 30 first patients is 24.4 μg/g (±20%, 1 SD) using a 6 h infusion of boronophenylalanine (BPA). It was reasonable to use a homogeneous brain–boron concentration of 25 μg/g ^{10}B in the present calculations, assuming a blood-to-healthy tissue ratio of about unity (33). The ICP-AES measurements of the boron concentration in the blood were followed as a function of time using a method presented previously (2, 34).

Figure 1 shows two alternatives regarding the irradiation geometry, i.e. treatment fields of the 'Side' or 'Top' field. In clinical reality, it was not always apparent whether a treatment field was a 'Side' or 'Top field', which introduces

Table 2

Summary of the absorbed dose and wire activation ratios calculated for the different materials and geometries under consideration (each parameter is normalized separately to unity for the reference conditions). The 'thermal neutron fluence' refers to the neutron fluence in the 0–0.414 eV energy interval. The thermal neutron (group) fluence rate can be converted to absorbed dose by multiplication of 1.84×10^{-12} Gy cm^2 (for 25 μg/g boron) and 1.50×10^{-13} for nitrogen, respectively. The statistical uncertainties of the parameters calculated were less than 2%, except for the fast neutron dose, which was 3%

Quantity	Reference conditions	Snyder model (top field)	Snyder model (side field)
Actovatopm rate [1]	1.000	0.769	0.870
Activation rate [2]	1.000	0.793	0.883
Photon dose	1.000	0.845	1.036
Fast neutron dose	1.000	1.319	1.318
Thermal neutron fluence	1.000	0.758	0.860

an additional uncertainty. The simulations show that the absorbed dose rate in the 'Side field' geometry was about 16% higher than the 'Top field' for the boron concentration used in the calculations. In the instance that the treatment field was something in between 'Side' or 'Top', a deviation from the reference value of up to half that amount (i.e. $\pm$8%) can be expected for geometric reasons for an individual treatment field. This was chosen as the action level indicating the need for further investigation. ICRU (15) recommended 5% as an aim for the overall accuracy of radiotherapy dosimetry. Choosing a tolerance of $\pm$5% in the present study would result in the inconvenience of conducting investigations on a large fraction of the treatment fields that are to be delivered. Note that the recommendation of the ICRU pertaining to the absorbed dose delivered is that it should be within $\pm$5% of the prescription. Brahme et al. (35) suggested that dose delivery in photon and electron therapy be delivered with an uncertainty of no more than 3% (1SD) in general for curative treatments. Mijnheer et al. (36) proposed that the uncertainty of the dose delivery should be no more than 7.0% (2 SD) in both photon and fast neutron therapy, although it was also concluded that this was not attainable in a typical parallel-opposed beam arrangement in neutron therapy. The uncertainty of the dose delivery in a parallel-opposed beam arrangement was 6.4% and 8.0% (1SD) for two different beam qualities. No similar analysis has been performed for BNCT presently to the author's knowledge, thus it seems reasonable to adopt the aim of 7.0% (2 SD) total uncertainty in the dose delivery given by Mijnheer et al. (36) until further information is available, even though it may be difficult to realize in reality. Seppälä et al. provided a thorough uncertainty analysis for the dosimetry of an animal study at the Finnish BNCT facility (24), which provides an insight into the dosimetric uncertainties in epithermal neutron beams in general.

The information in Tables 1 and 2 allows calculation of the absorbed dose delivered to a point (reference dose value—dose at the maximum) in a patient undergoing BNCT. The total uncertainty of the reference dose value was estimated at 6.0% (1 SD), including uncertainties related to the MCNP model (2.3%, 1 SD), the geometry of the patient (3.9%, 1 SD), the actual distance from the neutron beam (3.3%, 1 SD), and the calibration under reference conditions (1.5%, 1 SD). The uncertainty introduced by the assumptions regarding the boron and nitrogen tissue concentrations and distributions was omitted. The deviations between the TPS calculations and the reference dose value were on average 0.3%, and the spread around this average was $\pm$4.2% (1 SD) for the first 30 patients and for the total of 60 treatment fields. Two of the treatment fields fell outside the action level for further investigation. Both treatment fields were somewhat difficult to judge in terms of whether they were of the 'Side' or 'Top' type, and, when comparing with the average of the reference dose values for the two geometries, deviations of only about 1% were obtained. Therefore, these deviations were no cause for concern in the clinical process.

It is likely that the deviations found in comparison between the reference dose value and the TPS value were largely explained by geometric factors, considering the rather large difference between the two geometries studied here. A difference between the MCNP model and the TPS model was that the TPS makes use of a voxel-based representation of the geometry, while the MCNP model was an analytical description. The effect of the size of the voxels in a TPS used for BNCT has recently been investigated (37); the present TPS utilizes $5 \times 5 \times 5$ mm^3 voxels. Also the geometric description of the phantom used will have an impact in the present situation; we have here chosen an ellipsoidal volume of brain tissue with simplified representations of skull and scalp, which is a rather crude approximation of a human head. An added complexity in the Snyder model, for instance by introducing more compartments, seems unjustified, given the comparatively large uncertainty related to the simplification associated with these geometrical effects. The comparison performed in this study suggests that the simplified model used here was good enough for the present application, as the TPS calculated doses at the maximum in tissue were generally in rather good agreement with the reference dose values. In the future, it is of interest to expand the QA process to check the absorbed dose determined at the prescription point for the treatment planning calculations, where all treatment fields are added with their respective field weights. A method for performing this was recently demonstrated for photon radiotherapy (38).

In vivo dosimetry

From the information in Table 2 it is clear that the activity of the wire is a rather good measure of the boron and nitrogen dose components (assuming that the weight concentration of these materials is known) as the as the thermal neutron fluence per wire activity decrease similarly in both types of irradiation geometries compared with reference conditions. Therefore, the errors introduced due to the field set-up (i.e. division into the two standard 'Side' and 'Top' fields) will be low, as the difference in dose rate will be represented similarly in the induced activity in the wire, which suggests that the wire activity was largely affected by back-scattering neutrons. However, the photon and fast neutron dose-per-activity was about 10% different in the two geometries. As can be seen in Table 2, the fast neutron dose was more or less the same regardless of the geometry (for the same material). Considering that the product of the conversion factors in equation 4 was rather similar in the two geometries ('Top' or 'Side' field) it was reasonable to

use the same factors (the average) to simplify the evaluation process, which was done subsequently for the in vivo dosimetry.

We have evaluated the agreement between the TPS and in vivo dosimetry measurements of the total absorbed dose at the dose maximum (entrance dose). An average deviation of +3.9% was found (Measured/TPS-1) with a standard deviation of ±12% (1 SD). The maximum deviation between the TPS planned and the measured was +31% and −23% (Measured/TPS-1), respectively. The in vivo dosimetry system presented here indicates that actual deviations between the planned and delivered treatment are significantly larger than the recommended ±7.0% by Mijnheer et al. (36) had occurred in several instances. There was no correlation between the deviations of the in vivo dosimetry measurements/TPS and those found in the reference dose value/TPS comparisons. The comparatively small deviation found in the reference dose value/TPS comparisons suggests that the treatment planning calculations were correct, within stated uncertainties, and the deviations found were due to other reasons.

The total uncertainty of the in vivo dosimetry system was estimated to be 5.5% (1 SD), including an uncertainty of 2.6% related to the MCNP model (1.6% type A and 2.0% estimated type B uncertainty), and an estimated uncertainty of 2.3% (1 SD) related to the beam calibration performed on the PMMA phantom, and an 'experimental' uncertainty of 4.4% (1 SD) referring to the placement of the wire on the patient as well as to the calibration of the system. The 'experimental' uncertainty includes the effects of placing the wire accidentally off-axis. Assuming a 5 mm off-axis mispositioning reduces the induced activity by about 3% (assumed to correspond to 1 SD), and the read-out procedure of the wire activity (±1.0%, 1 SD), gives an uncertainty related to the calibration of the in vivo dosimetry system of 3% (1 SD) and an uncertainty of 2% (1 SD) related to the assumption of the boron concentration. The uncertainty regarding the boron concentration was estimated by performing one additional calculation in the 'Side' geometry case, with the skull and scalp compartment present, but with an average boron concentration of 10 μg/g ^{10}B in the brain tissue compartment instead of 25 as used in the other calculations in the present study. The calculation yielded increased wire activity, +2% (±1%, 1 SD), and increased thermal neutron fluence at the reference point: +5.1% (±0.4%, 1 SD). At a glance, it could be considered prudent to overestimate the brain-to-blood boron concentration ratio in the TPS calculations in the sense that the boron dose to the brain will be overestimated. On the other hand, the procedure also introduces a risk of underestimating the boron dose to the blood vessels due to an overestimated suppression of the thermal neutron fluence in the treatment planning calculations.

In the use of the system, we observed that in some instances the patient's hair and the aqua-plastic mask used to fixate the patient made it difficult to place the activation wire directly on the patient's skin. In addition, a collimator to skin distance of between 0 and 1 cm was employed, while in the in vivo dosimetry system described herein, we assumed a zero collimator to skin distance. These two effects were estimated experimentally, yielding a decrease of about 7% in the wire activity for a 2 mm gap between the wire and the surface of the phantom, and about 6% increase in the wire activity per thermal neutron fluence at the reference point for a collimator distance of 0.5 cm compared with zero. Including these two experimentally determined uncertainties (and assuming that they correspond to one standard deviation) yields a total estimated uncertainty of 11.2%, which is comparable to the observed deviations of the in vivo dosimetry measurements. Unfortunately, it was difficult to correct for the uncertainties introduced. A possible improvement of the in vivo dosimetry system may be an introduction of a 'build-up cap' for the activation wire, which might reduce the effect of having a gap between the wire and the skin, although such a cap could possibly spoil the skin-sparing effect of the depth dose build-up which would then require investigation. A high-purity germanium crystal was used to measure gold and copper activities of the activation wires. The statistical uncertainties of the gamma lines used to evaluate gold activity were about 1% (1 SD); the copper lines used are rather weak, therefore they were only used as an extra check that no obvious mistakes were made in the activation analysis. In the present set-up, low activation was induced in the gold–copper alloy wires, which made the readout rather time-consuming. The advantage was that the wires contain so little material that the radiation field was insignificantly perturbed by its presence.

The in vivo dosimetry method described previously by Seppälä et al. (24) requires information regarding the treatment time for a delivered field for the subsequent calculation of the saturated activity of the activation wires, which was used to determine the thermal neutron fluence at the skin surface. In general, it is inappropriate for an in vivo dosimetry system to require knowledge of the treatment time, as the method then relies on the very data that are to be verified. Using the method presented here, on the other hand, the in vivo dosimeters were calibrated in order to provide an estimate of the delivered dose at the dose maximum of each treatment field, and no knowledge of the treatment time was needed.

The deviations could be due to the method employed, involving comparisons of absorbed dose and fluence rates in interface (high gradient) regions (24). In addition, it is quite possible that variations in the sensitivity of the TL/foil detectors with photon/neutron spectra introduced additional uncertainties in the reported measurements.

The very high deviations shown in the TLD measurements indicate that the use of this detector as a tool for in vivo dosimetry in BNCT is questionable. However, the use of TLDs may still have an application in the acceptance phase of a facility when the whole body dose burden of BNCT patients needs investigation. In the possible event of a substantial increase in life expectancy of BNCT patients, the whole body dose burden may be a parameter of clinical interest.

CONCLUSION

The verification of the absorbed dose shows that the irradiation geometry of the patient has a clear impact on the absorbed dose to a reference point. It is still worthwhile to check the number of monitor units that are to be delivered using the rather simple methodology presented in this study. We have evaluated the agreement between the TPS and this independent calculation model. An average deviation of $+0.3\%$ was found with a standard deviation of 4.2% in the independent check prior to therapy, using a division of treatment fields into two standard cases. In the present study, a point at the dose maximum was checked for each individual treatment field.

The in vivo dosimetry studied showed unsatisfactorily large deviations between the planned and delivered absorbed dose that would be satisfactory ($\pm 12\%$, 1SD). These deviations were unlikely to represent real deviations in patient dosimetry as they are similar to the estimated uncertainty of the system, but signify the need for further improvements. The in vivo dosimetry system presented in this study still shows a level of agreement that appears to be somewhat better than previously reported for an epithermal neutron beam (24); however, the methods used and the parameters verified were different.

The present study shows that QA systems for BNCT dosimetry can be implemented and used with small effort and costs that provide a good starting point for additional studies. One of the inherent drawbacks of using activation wires as in vivo dosimeters is that the results of the measurements are acquired in post-analysis. The method presented herein avoids this problem by performing an independent check of the dosimetry prior to each treatment. In this respect a complete quality assurance system for patient dosimetry in BNCT is presented in this study.

ACKNOWLEDGEMENTS

The authors would like to thank Studsvik Medical AB, the Wallenberg foundation, the Swedish Cancer foundation, John and Augusta Persson's foundation, the Swedish House of Nobility and the Gunnar Nilsson foundation for financial support. Los Alamos National Laboratory is acknowledged for providing the MCNP code. Dr Britta H.-Stenstam and Prof. Kurt Sköld are acknowledged for their support of this study. Eva Wallin is acknowledged for technical support.

REFERENCES

1. Giusti V, Munck af Rosenschöld PM, Sköld K, Montagnini B, Capala J. Monte Carlo model of the Studsvik BNCT facility: description and validation. Med Phys 2003; 30: 3107–17.
2. Capala J, H.-Stenstam B, Sköld K, Munck af Rosenschöld PM, Giusti V, Persson C, Wallin E, Brun A, Franzen L, Carlsson J, Salford LG, Ceberg C, Persson BRR, Pellettieri L, Henriksson R. Boron neutron capture therapy for glioblastoma multiforme: clinical studies in Sweden. J Neuro-Oncol 2003; 62: 135–44.
3. Svensson H, Moller TR. Developments in radiotherapy (SBU Survey Group). Acta Oncol 2003; 42(5–6): 430–42.
4. Carlsson J, Forssell-Aronsson E, Glimelius B. Radiation therapy through activation of stable nuclides. Acta Oncol 2002; 41: 629–34.
5. Coderre JA, Morris GM. The radiation biology of boron neutron capture therapy. Radiat Res 1999; 151: 1–18.
6. Kosunen A, Kortesniemi M, Ylä-Mella H, Seppälä T, Lampinen J, Serén T, Auterinen I, Järvinen H, Savolainen S. Twin ionization chambers for dose determinations in phantom in an epithermal neutron beam. Rad Prot Dos 1999; 81: 187–94.
7. Liu HB, Greenberg DD, Capala J, Wheeler FJ. An improved neutron collimator for brain tumor irradiations in clinical boron neutron capture therapy. Med Phys 1996; 23: 2051–60.
8. Raaijmakers CPJ, Konijnenberg MW, Verhagen HW, Mijnheer BJ. Determination of dose components in an epithermal neutron beam for boron neutron capture therapy. Med Phys 1995; 22: 321–9.
9. Rogus RD, Harling OK, Yanch JC. Mixed field dosimetry of epithermal neutron beams for boron neutron capture therapy at the MITR-II research reactor. Med Phys 1994; 21: 1611–25.
10. Munck af Rosenschöld PM, Ceberg CP, Giusti V, Andreo P. Photon quality correction factors for ionization chambers in an epithermal neutron beam. Phys Med Biol 2002; 47: 2397–409.
11. Munck af Rosenschöld PM, Giusti V, Ceberg CP, Capala J, Sköld K, Persson BRR. Reference dosimetry at the neutron capture therapy facility at Studsvik. Med Phys 2003; 30: 1569–79.
12. Raaijmakers CPJ, Nottelman EL, Mijnheer BJ. Phantom materials for boron neutron capture therapy. Phys Med Biol 2000; 45: 2353–61.
13. Seppälä T, Vähätalo V, Auterinen I, Kosunen A, Nigg DW, Wheeler FJ, Savolainen S. Modelling of brain tissue substitutes for phantom materials in neutron capture therapy (NCT) dosimetry. Radiat Phys Chem 1999; 55: 239–46.
14. Harling OK, Roberts RA, Moulin DJ, Rogus RD. Head phantoms for boron neutron capture therapy. Med Phys 1995; 22: 579–83.
15. International Commission on Radiation Units and Measurements. Determination of absorbed dose in a patient irradiated by beams of X or gamma rays in radiotherapy procedures. ICRU Report No. 24. Bethesda, MD: ICRU Publications; 1976.
16. Kutcher GJ, Coia L, Gillin M, Hanson WF, Leibel S, Morton RJ, Palta JR, Purdy JA, Reinstein LE, Svensson GK, Weller M, Wingfield L. Comprehensive QA for radiation oncology: report of AAPM Radiation Therapy Committee Task Group 40. Med Phys 1994; 21: 581–618.
17. Van Dam J, Marinello G. Methods for in-vivo dosimetry in external radiotherapy determination of absorbed dose in a patient irradiated by beams of X or gamma rays in radiotherapy procedures. ESTRO document, 1994, ISBN 90 5350 298 X.
18. Kobayashi T, Sakurai Y, Ishikawa M. A noninvasive dose estimation system for clinical BNCT based on PG-SPECT—

conceptual study and fundamental experiments using HPGe and CdTe semiconductor detectors. Med Phys 2000; 27: 2124–32.
19. Munck af Rosenschöld PM, Verbakel WF, Ceberg CP, Stecher-Rasmussen F, Persson BRR. Toward clinical application of prompt gamma spectroscopy for in-vivo monitoring of boron uptake in boron neutron capture therapy. Med Phys 2001; 28: 787–95.
20. Verbakel WFAR. Validation of the scanning-gamma-ray telescope for in vivo dosimetry and boron measurements during BNCT. Phys Med Biol 2001; 46: 3269–85.
21. International Commission on Radiation Units and Measurements. Clinical neutron dosimetry, Part I: determination of absorbed dose in a patient treated by external beams of fast neutrons. ICRU Report No. 45. Bethesda, MD: ICRU Publications; 1989.
22. Rassow J, Stecher-Rasmussen F, Voorbraak W, Moss R, Vroegindeweij C, Hideghéty K, Sauerwien W. Comparison of quality assurance for performance and safety characteristics for boron neutron capture therapy in Petten/NL with medical electron accelerators. Rad Oncol 2001; 59: 99–108.
23. Aschan C, Serén T, Seppälä T, Benczik J, Toivonen M, Auterinen I, Savolainen S. In-vivo dosimetry of the dog irradiations at the Finnish BNCT facility. Frontiers in Neutron Capture Therapy 2001, ISBN 0 306 46442 X.
24. Seppälä T, Auterinen I, Aschan C, Serén T, Benczik J, Snellman M, Huiskamp R, Ramadan UA, Kankaranta L, Joensuu H, Savolainen S. In-vivo dosimetry of the dog irradiations at the Finnish BNCT facility. Med Phys 2002; 29: 2629–40.
25. Salford LG, Brun A, Nirfalk S. Ten-year survival among patients with supratentorial astrocytomas grade III and IV. J Neurosurg 1988; 69: 506–9.
26. Kiger WS III, Sakamoto S, Harling OK. Neutronic design of a fission converter-based epithermal neutron beam for neutron capture therapy. Nuc Sci Eng 1999; 131: 1–22.
27. Briesmeister JF, MCNP—a General Monte Carlo N-Particle Transport Code, Version 4C, LA-12625-M. Los Alamos, NM: Los Alamos National Laboratory; 2000.
28. Fukuda H, Hiratsuka J, Honda C, Kobayashi T, Yoshino K, Karashima H, Takahashi J, Abe Y, Kanda K, Ichihashi M, Mishima Y. Boron neutron capture therapy of malignant melanoma using ^{10}B-paraboronophenylalanine with special reference to the evaluation of the radiation dose and damage to the normal skin. Rad Res 1994; 138: 435–42.
29. IAEA. Current status of neutron capture therapy. Technical Report Document No. 1223. Vienna: IAEA; 2000, ISSN 1011 4289.
30. Nigg DW, Wheeler FJ, Wessol DE, Capala J, Chadha M. Computational dosimetry and treatment planning for boron neutron capture therapy." J. Neuro-Oncol 1997; 33: 93–104.
31. Wessol DE, Wheeler FJ. Creating and using a type of free-form geometry in Monte Carlo Particle Transport. Nucl Sci Eng 1993; 113: 314–23.
32. Wheeler FJ, Nigg DW. Three-dimensional radiation dose distribution analysis for boron neutron capture therapy. Nucl Sci Eng 1992; 110: 16–31.
33. Elowitz EH, Bergland RM, Coderre JA, Joel DD, Chadha M, Chanana AD. Biodistribution of *p*-boronophenylalanine in patients with glioblastoma multiforme for use in boron neutron capture therapy. J Neurosurg 1998; 42: 463–9.
34. Ryynanen PM, Kortesniemi M, Coderre JA, Diaz AZ, Hiismaki P, Savolainen S. Models for estimation of the (10)B concentration after BPA–fructose complex infusion in patients during epithermal neutron irradiation in BNCT. Int J Radiat Oncol Biol Phys 2000; 48: 1145–54.
35. Brahme A, et al. Accuracy requirements and quality assurance of external beam therapy with photons and electrons. Acta Oncol 1988 (Suppl 1).
36. Mijnheer BJ, Battermann JJ, Wambersie A. What degree of accuracy is required and can be achieved in photon and neutron therapy? Radiother Oncol 1987; 8: 237–52.
37. Goorley JT, Kiger WS III, Zamenhof RG. Reference dosimetry calculations for neutron capture therapy with comparison of analytical and voxel models. Med Phys 2000; 29: 145–56.
38. Knöös T, Johnsson SA, Ceberg CP, Tomaszewicz A, Nilsson P. Independent check of the delivered dose for high-energy X-rays using a hand-held PC. Radiother Oncol 2001; 58: 201–8.